

Detailed calculation and analysis of electrical properties in solution-processed polymer semiconducting layers

LI-GUO WANG*, HUAI-WU ZHANG, XIAO-LI TANG, YUAN-QIANG SONG

State Key Laboratory of Electronic Thin Films and Integrated Devices, University of Electronic Science and Technology of China, Chengdu, 610054, China

Recently, it has been demonstrated that the extended Gaussian disorder model (EGDM) can well describe the current-voltage ($J - V$) characteristics of hole-only devices of PPV-based polymers. In this paper, we propose a useful numerical method adopting the uneven discretization and Newton Iteration Method to solve the coupled equations describing the space-charge limited (SCL) current in conjugated polymers. Based on this numerical method and the extended Gaussian disorder model, we calculate and analyze some electrical properties of solution-processed poly[2-methoxy-5-(2'-ethylhexyloxy)-*p*-phenylene vinylene] (MEH-PPV) in detail. We show that the boundary carrier density has an important influence on the current-voltage characteristics. Too large or too small values of the boundary carrier density will lead to incorrect current-voltage characteristics. Additionally, it is shown that the numerically calculated carrier density is a decreasing function of the distance from the interface and numerically calculated electric field is an increasing function of the distance. The maximum of carrier density and the minimum of electric field appear near the interface.

(Received August 17, 2010; accepted March 16, 2011)

Keywords: Organic semiconductors, Electrical properties, Extended Gaussian disorder model, Numerical method

1. Introduction

In the past decade solution-processable organic semiconductors have received much attention due to their potential for optoelectronic applications as polymer light-emitting diodes (PLEDs) [1, 2]. It is of crucial importance to understand the charge transport in these materials in order to design and synthesize better materials and improve device performances. The most important parameters in this transport is the charge carrier mobility μ , which quantifies how easily charge carriers move when an electric field is applied. In particular, the dependence of μ on temperature T and electric field E has been extensively investigated [3-11]. Charge transport in these disordered semiconducting polymers has been described by hopping of charge carriers from one localized state at a specific site to another. The variations in the one-site energies due to disorder are usually taken to be Gaussian. Within the pioneering Monte Carlo studies of the effects of disorder on the mobility, Bässler and co-workers introduced a model with an uncorrelated Gaussian distribution of hopping site energies, which is known as the "Gaussian disorder model" (GDM) [3, 4]. Their results showed a non-Arrhenius temperature dependence of the mobility $\mu \propto \exp(-(2\sigma/3kT)^2)$ and a Poole-Frenkel behavior $\mu \propto \exp(\gamma\sqrt{E})$ for the electric-field dependence in a rather limited field range. Gartstein and conwell argued that in order to obtain a Poole-Frenkel behavior in a broad range of field strengths,

it is necessary to assume correlation between the site energies, leading to the "correlated disorder model" (CDM) [8].

Recently, it was realized that the importance of the charge carrier density p had been overlooked [12, 13]. The experimental hole mobilities extracted from hole-only diodes and field-effect transistors, although based on the same polymeric semiconductor, can differ by 3 orders of magnitude [13]. It was demonstrated that this apparent discrepancy originates from the strong dependence of the hole mobility on the charge carrier density in disordered semiconducting polymers. More recent experiments suggested that it is sufficient to take only the p dependence of μ into account at room temperature, but that at low temperatures it is still necessary to assume an E dependence [14]. These experiments revealed that for a complete description of the charge transport in disordered semiconducting polymers, a model that incorporates both the effect of the carrier density and electric field on the mobility is required. Based on these observations, Pasveer *et al.* showed that an extension of the GDM to include a carrier density dependence of the mobility, leading to the "extended Gaussian disorder model" (EGDM), can well describe the temperature dependent current-voltage characteristics $J(V, T)$ of hole transport in sandwich-type devices based on polyphenylene-vinylene (PPV) polymers [15]. A similar conclusion was obtained by van Mensfoort *et al.*, who analyzed the $J(V, T)$ characteristics of hole-only

polyfluorene-based copolymer devices with various layer thicknesses [16]. It has been demonstrated that the extended Gaussian disorder model (EGDM) is more applicable for disordered organic semiconductors than the commonly used model within which the mobility depends only on the electric field.

It is worth noting that some electrical properties of solution-processed conjugated polymers have not been studied so far, including the variation of current-voltage ($J-V$) characteristics with the boundary carrier density and the distribution of the charge carrier density and electric field with the distance from the interface. These properties are also essential to synthesize better materials and improve the device performances. In this paper, we propose a useful numerical method using the uneven discretization and Newton Iteration Method to solve the coupled equations describing the space-charge limited (SCL) current in conjugated polymers. Based on this numerical method and the extended Gaussian disorder model, we calculate and analyze these electrical properties of solution-processed poly[2-methoxy-5-(2'-ethylhexyloxy)-*p*-phenylene vinylene] (MEH-PPV) in detail. In Sec. 2 the extended Gaussian disorder model that determines the dependence of charge carrier mobility on temperature, carrier density, and electric field is outlined, and our calculational method used is presented. In Sec. 3 the main numerical results and discussions are presented. Sec. 4 contains a summary and conclusions.

2. Model and methods

Recent studies have demonstrated that the hole mobility MEH-PPV is dependent on the carrier density p , the applied electric field E , and temperature T [13, 14]. The carrier density dependence of the mobility dominates the SCL $J-V$ characteristics at room temperature, whereas the field-dependence becomes more important at lower temperature. From a numerical solution of the master equation for hopping transport in a disordered energy system with a Gaussian density of states (DOS) a charge transport model has been developed by Pasveer *et al.* that determines the dependence of the charge carrier mobility μ on the carrier density p , the electric field E , and temperature T [15]. It has been demonstrated that the mobility can be described as:

$$\mu(T, p, E) \approx \mu(T, p)f(T, E), \quad (1)$$

$$\mu(T, p) = \mu_0(T) \exp\left[\frac{1}{2}(\hat{\sigma}^2 - \hat{\sigma})(2pa^3)^\delta\right], \quad (2)$$

$$\mu_0(T) = \mu_0 c_1 \exp(-c_2 \hat{\sigma}^2), \quad (3)$$

$$\delta \equiv 2\hat{\sigma}^{-2}[\ln(\hat{\sigma}^2 - \hat{\sigma}) - \ln(\ln 4)], \quad (4)$$

$$\mu_0 \equiv \frac{a^2 v_0 e}{\sigma}, \quad (5)$$

$$f(T, E) = \exp\left\{0.44(\hat{\sigma}^{3/2} - 2.2)\left[\sqrt{1 + 0.8\left(\frac{eaE}{\sigma}\right)^2} - 1\right]\right\}. \quad (6)$$

with $c_1 = 1.8 \times 10^{-9}$ and $c_2 = 0.42$. Where $\mu_0(T)$ is the mobility in the limit of zero charge carrier density and zero electric field, $\hat{\sigma} \equiv \sigma/k_B T$ and σ is the width of the Gaussian density of states (DOS), a is the lattice constant, e is the charge of the carriers, and v_0 is an attempt frequency, $f(T, E)$ is the field-dependent mobility factor.

Using the above model, the $J-V$ characteristics and some other electrical properties of conjugated polymers can be obtained by numerically solving the following coupled equations.

$$J = p(x)e\mu(T, p(x), E(x))E(x), \quad (7)$$

$$\frac{dE}{dx} = \frac{e}{\varepsilon_0 \varepsilon_r} p(x), \quad (8)$$

$$V = \int_0^L E(x) dx, \quad (9)$$

where x is the distance from the injecting electrode, L is the polymer layer thickness sandwiched between two electrodes, ε_0 is the vacuum permeability, and ε_r is the relative dielectric constant of the polymer.

It is obvious that Eqs. (7)-(9) are non-linear integro-differential equation. In order to solve these equations, we present a particular discretizing approach. First we discretize Eqs. (7)-(9) by dividing the thickness L into n segments as follows (we take $n = 8000$ in the calculations)

$$\Delta x = L/n^m, \quad x_i = i^m \Delta x, \quad i = 0, \dots, n. \quad (10)$$

The values of $p(x)$ and $E(x)$ are represented as

$$p_i = p(x_i), \quad E_i = E(x_i). \quad (11)$$

Then Eqs. (7)-(9) can be transformed to the following form

$$J = ep_i \mu(T, p_i, E_i) E_i, \quad (12)$$

$$\frac{(E_{i+1} - E_i)}{[(i+1)^m - i^m] \Delta x} = \frac{e}{\varepsilon_r \varepsilon_0} p_i, \quad (13)$$

$$V = \frac{1}{2} \Delta x \sum_{i=1}^n (E_i + E_{i-1}) [i^m - (i-1)^m], \quad (14)$$

where Eq. (13) is from Eq. (8) by adopting the numerical

differential and Eq. (14) is from Eq. (9) by adopting the trapezoid integrating approach.

It can be seen from Eqs. (12)-(14) that, for a given T and J , the corresponding value of V can be easily obtained as the following procedure. Firstly, we assume a value of p_0 for a given T and J . Subsequently, we solve E_0 from Eq. (12) by using Newton Iterative Method. Then we can repeat the following two steps n times ($i = 0 \sim (n-1)$): evaluating E_{i+1} from Eq. (13) and solving p_{i+1} from Eq. (12) by Newton Iterative Method again. Finally, once all values of E_i ($i = 0 \sim n$) are evaluated, the voltage V can be easily obtained from Eq. (14).

3. Results and discussion

By using the extended Gaussian disorder model and our calculational method as described in Sec. 2, we now calculate and analyze the electrical properties for polymer layer of MEH-PPV with layer thickness $L = 160$ nm in detail. The other parameters we adopt the following values as determined by Zhang *et al.* in Ref. [17], $a = 1.55$ nm, $\sigma = 0.143$ eV, $\mu_0 = 6400$ m²/V s.

It should be noted that the boundary carrier density (the carrier density at the interface) $p(0) = p_0$ is very important in the calculations, which can affect the current-voltage ($J-V$) characteristics. Thus it is necessary to analyze the influence of the boundary carrier density $p(0)$ on the $J-V$ characteristics. The variation of the $J-V$ characteristics with $p(0)$ at low temperature and room temperature for MEH-PPV are plotted in Fig. 1. The figure shows that the voltage is an increasing function of the current-density, and the variation of voltage with $p(0)$ is dependent on the current-density. The voltage decreases with increasing $p(0)$ for enough small value of $p(0)$, and the voltage shows a steep decrease with increasing current-density. On the other hand, the voltage also increases with increasing $p(0)$ for sufficiently large value of $p(0)$, and the voltage shows a steep increase with decreasing current-density. Nevertheless, it is worth noting that in the middle regions, the $V-p(0)$ curves are fairly flat. This means that the voltage is almost independent on $p(0)$ in this region. As a result, too large or too small values of $p(0)$ lead to incorrect $J-V$ characteristics, and the values of $p(0)$ in the middle region can achieve reasonable results. The physical reason of variation in Fig. 1 can be understood as follows: At small $p(0)$ region, the concentration of charge carriers in bulk materials is small, the impedance and voltage are relative large. As the $p(0)$ increasing into the middle region, the carriers injection near the interface and the drain into the bulk materials will reach equilibrium, the $J-V$ characteristics move into the Ohmic region, and the $V-p(0)$ curves become flat. In order to further verify this point, we compare the calculated $J-V$ characteristics with the experimental results from Ref. [17] with the values of

$p(0)$ in the middle region in Fig. 2. The figure shows a very good agreement between the numerically calculated results and experimental data. Otherwise, the calculated $J-V$ characteristics will deviate from the experiment as the values of $p(0)$ is not taken in the middle region.

It is clear from Fig. 1 that, in order to reach the same current-density J at the same charge carrier density $p(0)$, the stronger electric field and corresponding larger voltage is needed at low temperature than that at high temperature. As for this point, it is generally agreed that the thermal excitation and the energy of carriers motion in conjugated polymers is relatively weaker at low temperature than that at high temperature. Thus we can conclude that the charge carrier density dominates the SCL $J-V$ characteristics at room temperature, and the electric field becomes more important at lower temperature. These conclusions are fully consistent with the earlier reported results of Tanase *et al.* [14] and Pasveer *et al.* [15].

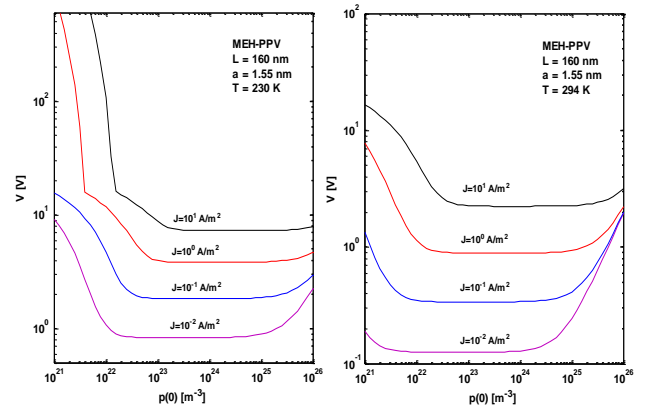


Fig. 1. Theoretical results of voltage versus the boundary carrier density for polymer layers of MEH-PPV at 230 K and 294 K, respectively. Different Lines correspond to different current density values, J in unit A/m².

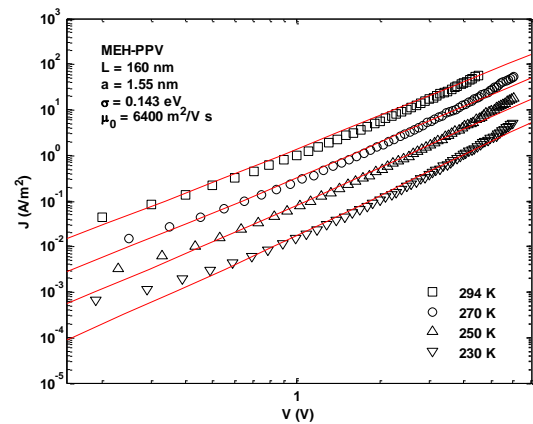


Fig. 2. Current density versus voltage characteristics of MEH-PPV hole-only device with a thickness of 160 nm for various temperatures. Full lines: numerical solution of Eqs. (7)-(9) with T , p and E dependent mobility from Eqs. (1)-(6). Symbols: experimental results from Ref. [17].

In Fig. 3, we display the calculated results of the carrier density as a function of the distance from the interface within the polymer layer for MEH-PPV at 230 K and 294 K with $J = 0.01$ and 1.0 A/m^2 . As shown already above, the calculated $J-V$ characteristics are in accordance with that of Zhang *et al.* [17] only when the value of $p(0)$ is taken in the middle region. Thus we take two values of $p(0)$, $(0.1, 1) \times 10^{23} \text{ m}^{-3}$, for MEH-PPV in the calculations, which belong to the middle region. The figure shows that the carrier density $p(x)$ is a decreasing function of the distance x . The speed of decrease is rapid for the cases with large values of $p(0)$. On the other hand, the speed of decrease is slow for small values of $p(0)$, and the corresponding curves are flat. As the distance x increasing, $p(x)$ rapidly reaches the saturated values in the bulk. Moreover, the figure also shows that the thickness of accumulation layer is a function of the boundary carrier density. The larger the value of $p(0)$ is, the smaller the thickness of accumulation layer is, vice versa. These calculated results are qualitatively in agreement with the simulated results of Demeyu *et al.* [18] and the experimental measurements of Kiguchi *et al.* [19].

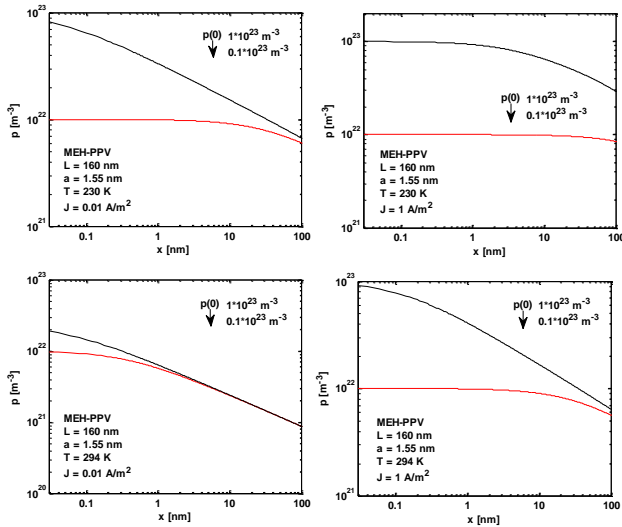


Fig. 3. Numerically calculated distribution of charge carrier density p as a function of position x in a hole-only device based on MEH-PPV for low and high current densities at $T = 230 \text{ K}$ and 294 K .

In Fig. 4, we display the calculated results of the electric field as a function of the distance for MEH-PPV. The figure shows that the electric field E is an increasing function of the distance x and the shape of $E-x$ curves are similar to the reflection of $p-x$ curves shown in Fig. 3. The speed of increase is rapid for the cases with large values of $p(0)$, and is slow for the cases with small values of $p(0)$. The thickness of accumulation layer deduced from Fig. 4 is in agreement with Fig. 3.

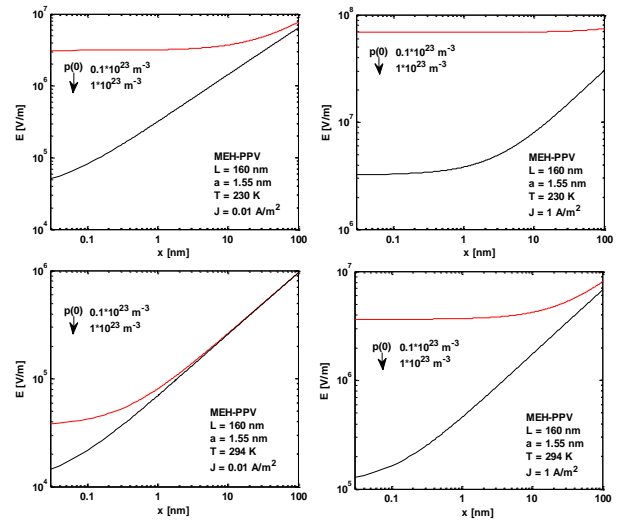


Fig. 4. Numerically calculated distribution of electric field E as a function of position x in a hole-only device based on MEH-PPV for low and high current densities at $T = 230 \text{ K}$ and 294 K .

Conclusively, the results on $p(x)$ and $E(x)$ presented in Fig. 3 and Fig. 4 clearly exhibit the SCL current density and voltage. Fig. 3 shows the space-charge distribution $p(x)$. The injection of carriers from electrode into polymer layer leads to carrier accumulation near the interface and decreasing function $p(x)$. The distribution $p(x)$ leads to the variation of $E(x)$, and the carrier accumulation near the interface results in increasing function $E(x)$ in terms of Poisson equation (Eq. (8)).

4. Summary and conclusions

We propose a useful numerical method adopting the uneven discretization and Newton Iteration Method to solve the coupled equations describing the space-charge limited (SCL) current in conjugated polymers. Based on this numerical method and the extended Gaussian disorder model, we calculate and analyze the variation of current-voltage ($J-V$) characteristics with the boundary carrier density and the distribution of the charge carrier density and electric field with the distance from the interface for MEH-PPV. It is shown that too large or too small values of the boundary carrier density lead to incorrect $J-V$ characteristics. Additionally, we show that the numerically calculated carrier density is a decreasing function of the distance from the interface and numerically calculated electric field is an increasing function of the distance. The maximum of carrier density and the minimum of electric field appear near the interface.

In conclusion, we demonstrate that the coupled equations combining the extended Gaussian disorder model can give reasonable description of the SCL current

density and voltage appeared in organic semiconductor devices. Relatively speaking, the charge carrier density dependence of the mobility dominates the SCL $J-V$ characteristics at room temperature, whereas the electric field-dependence becomes more important at lower temperature.

Acknowledgements

This work is partly supported by the National Basic Research Program of China (973) under Grant No. 2007CB31407, Foundation for Innovative Research Groups of the NSFC (Grant No. 60721001), the National Natural Science Foundation Grant No. 50972023, and the International S&T Cooperation Program of China under Grant No. 2006DFA53410 and 2007DFR10250.

References

- [1] J. H. Burroughes, D. D. C. Bradley, A. R. Brown, R. N. Marks, K. Mackay, R. H. Friend, P. L. Burns, A. B. Holmes, *Nature (London)* **347**, 539 (1990).
- [2] G. Gustafsson, Y. Cao, G. M. Treacy, F. Klavetter, N. Colaneri, A. J. Heeger, *Nature (London)* **357**, 477 (1992).
- [3] L. Pautmeier, R. Richert, H. Bässler, *Synth. Met.* **37**, 271 (1990).
- [4] H. Bässler, *Phys. Status Solidi B* **175**, 15 (1993).
- [5] P. W. M. Blom, M. J. M. de Jong, M. G. van Munster, *Phys. Rev. B* **55**, R656 (1997).
- [6] H. C. F. Martens, P. W. M. Blom, H. F. M. Schoo, *Phys. Rev. B* **61**, 7489 (2000).
- [7] Z. G. Yu, D. L. Smith, A. Saxena, R. L. Martin, A. R. Bishop, *Phys. Rev. Lett.* **84**, 721 (2000).
- [8] Y. N. Gartstein, E. M. Conwell, *Chem. Phys. Lett.* **245**, 351 (1995).
- [9] D. H. Dunlap, P. E. Parris, V. M. Kenkre, *Phys. Rev. Lett.* **77**, 542 (1996).
- [10] S. V. Novikov, D. H. Dunlap, V. M. Kenkre, P. E. Parris, A. V. Vannikov, *Phys. Rev. Lett.* **81**, 4472 (1998).
- [11] Y. Preezant, N. Tessler, *Phys. Rev. B* **74**, 235202 (2006).
- [12] Y. Roichman, N. Tessler, *Synth. Met.* **135**, 443 (2003).
- [13] C. Tanase, E. J. Meijer, P. W. M. Blom, D. M. de Leeuw, *Phys. Rev. Lett.* **91**, 216601 (2003).
- [14] C. Tanase, P. W. M. Blom, D. M. de Leeuw, *Phys. Rev. B* **70**, 193202 (2004).
- [15] W. F. Pasveer, J. Cottaar, C. Tanase, R. Coehoorn, P. A. Bobbert, P. W. M. Blom, D. M. deLeeuw, M. A. J. Michels, *Phys. Rev. Lett.* **94**, 206601 (2005).
- [16] S. L. M. van Mensfoort, S. I. E. Vulto, R. A. J. Janssen, R. Coehoorn, *Phys. Rev. B* **78**, 085208 (2008).
- [17] Y. Zhang, P. W. M. Blom, *Org. Electron.* **11**, 1261 (2010).
- [18] L. Demeyu, S. Sven, *Phys. Rev. B* **76**, 155202 (2007).
- [19] M. Kiguchi, M. Nakayama, T. Shimada, K. Saiki, *Phys. Rev. B* **71**, 035332 (2005).

* Corresponding author: wanglg23@uestc.edu.cn